

# Wall Pressure-Feeder Load Interactions in Mass Flow Hopper/Feeder Combinations

## Part II

**K.S. Manjunath and A.W. Roberts, Australia**

### Abstract

The interactive roles of mass flow bins and feeders are discussed. The effect of feeder speed, gate height, clearance between the hopper outlet and the feeder surface, method of filling, rate of filling on wall pressures in mass flow bins and feeder load and power requirements of the feeders are highlighted. Measurement of wall pressures suggests that initial pressures during filling are less than hydrostatic, hence initial loads on feeders are less than theoretically predicted. The higher experimental flow loads on the feeders are due to the fact that the measured values of wall pressures towards the vicinity of the outlet of the hopper diverge from the radial stress field theory of Jenike. On the basis of the above measurements, the values of  $K$  and  $n$  are computed and the bounds for initial filling are suggested. The flow loads are based on the major consolidating stress  $\sigma_1$ , which compares satisfactorily with the measured values. Finally, methods to control overloading of the feeders are discussed.

### Nomenclature

$a$	— gate height
$A$	— area
$B$	— hopper opening dimension and width between skirtplates
$B_b$	— belt width
$c$	— clearance between hopper and feeder
$D$	— bin diameter or width
$ff$	— flow factor
$F_a$	— force to accelerate material onto belt
$F_b$	— empty belt resistance
$F_{be}$	— belt load resistance, extended section beyond hopper
$F_{bh}$	— belt load resistance, hopper section
$F_t$	— tangential force, flow condition
$F_i$	— tangential force, initial condition

$F_s$	— skirtplate friction
$F_{spe}$	— skirtplate resistance, extended section beyond hopper
$F_{sph}$	— skirtplate resistance, hopper section
$g$	— acceleration due to gravity
$h_c$	— surcharge head acting at transition of cylinder and hopper
$h_o$	— distance from apex to transition of hopper
$h_s$	— bin surcharge head
$H$	— head of bulk solid in cylinder
$H_h$	— height of hopper
$H_s$	— actual bin surcharge
$K$	— ratio of $p_n/p_v$ for hopper
$K_j$	— pressure ratio in Janssen equation
$K_v$	— ratio of lateral to vertical pressure in skirtplate zone
$L$	— length of slotted hopper opening in plane flow bin
$L_c$	— length of conveyor
$L_s$	— length of skirtplates
$m$	— hopper shape factor; $m = 1$ for axisymmetric hopper, $m = 0$ for plane flow hopper
$m_c$	— cylinder shape factor; $m_c = 1$ for square or circular cylinder, $m_c = 0$ for rectangular cylinder
$m_s$	— surcharge factor; $m_s = 1$ for conical surcharge, $m_s = 0$ for triangular surcharge
$n$	— factor of index in bin pressure distribution equation
$p_n$	— normal wall pressure
$p_v$	— average vertical pressure
$P$	— power
$q$	— nondimensional surcharge factor
$q_t$	— nondimensional surcharge factor, flow condition
$q_{t\sigma_1}$	— nondimensional flow surcharge factor based on $\sigma_1$
$q_i$	— nondimensional surcharge factor, initial condition
$Q$	— feeder load
$Q_t$	— feeder load, flow condition
$Q_{t\sigma_1}$	— feeder load based on $\sigma_1$
$Q_i$	— feeder load, initial condition
$R$	— hydraulic radius
$v$	— belt velocity
$w_b$	— belt weight per unit length
$X, Y$	— factors in feeder load equations, flow condition
$y_e$	— depth of bulk solid in skirtplate zone, extended section
$y_h$	— depth of bulk solid in skirtplate zone, hopper section

Mr. K.S. Manjunath, Graduate Research Student, and Dr. A.W. Roberts, Professor, Head of Dept. and Dean of the Faculty of Engineering, University of Newcastle, Dept. of Mechanical Engineering, Newcastle, N.S.W. 2308, Australia.

Part I of this paper has been published in *bulk solids handling* Vol. 6 (1986) No.4, pp. 769–775.

- $z$  — depth coordinates in hopper
- $\alpha$  — hopper half-angle
- $\beta$  — angle in Eq. (17)
- $\gamma$  — bulk specific weight
- $\delta$  — effective angle of internal friction
- $\eta$  — drive efficiency
- $\mu$  — coefficient of friction
- $\mu_2$  — skirtplate friction coefficient
- $\mu_b$  — belt idler friction
- $\mu_i$  — coefficient of friction for bulk solid at feeder outlet
- $\xi$  — release angle
- $\rho$  — bulk density
- $\sigma_1$  — major consolidating pressure
- $\sigma_w$  — normal wall pressure
- $\phi$  — wall friction angle.

**7. Experimental Results and Discussion**

Experiments were conducted using the model perspex plane flow bin and flat bed belt feeder, as shown in Fig. 3, to examine the reliability of feeder load equations. Two bulk materials were handled, plastic pellets and white sand with different moisture contents. The effect of the filling rate, method of filling, feeder speed, gate height  $a$  and clearance  $c$  between the hopper outlet and the feeder surface on the feeder load, power requirements and wall pressures in the hopper have been investigated.

**7.1 Initial Filling Conditions**

In Fig. 9, the theoretical feeder loads as a function of the head  $H$  for the initial filling case have been plotted using Eq. (21) in conjunction with the nondimensional surcharge factor Eqs. (24), (25) and (26). In the case of Eq. (24), eight curves have been drawn for  $n = 0, 0.1, 0.2, 0.3, 0.4, 0.5, 1.5$  and  $3.0$ ; the curve based on  $n = 0$  is identical to that given by Eq. (25). The experimental results indicate that the initial feeder loads increase as the clearance between the hopper outlet and the feeder decreases; the larger clearance no doubt permits some redistribution of the pressure conditions at the outlet to provide a degree of cushioning. The influence of the rate of filling of the bin is quite significant; at the faster rate, the impact effect of the bulk solid discharging into the bin causes a greater degree of compaction.

Fig. 10 shows the theoretical feeder loads as a function of  $h_c$  for two types of filling: one filling directly from a chute and in the other case the chute feeding onto a distributor which evenly distributes the bulk solid along the length of the bin, as shown in Fig. 3. The hopper outlet was supported at two points which act as local stiffeners. The deflection of the skirt zone was recorded using linear voltage displacement transducers (LVDT).

Eqs. (24) to (27) and (29) have been plotted as shown. In the case of Eq. (24), curves have been drawn for the values of  $n = 0, 0.4, 0.5, 0.6, 0.7, 0.8, 0.9, 1.0$  and  $2.0$ .

The experimental results indicate that the initial feeder loads decrease as the bulk solid is evenly distributed using a distributor. This is due to the impact effects being absorbed in the distributor and the flow being uniform along the slot. Comparison of the experimental results with those based on

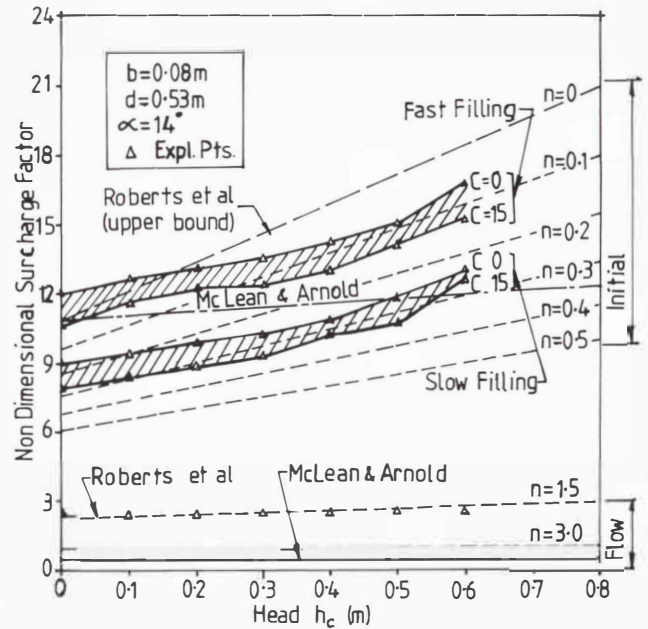


Fig. 9: Comparison of theoretical and experimental feeder loads in plane flow bin and belt feeder test rig — material: plastic pellets

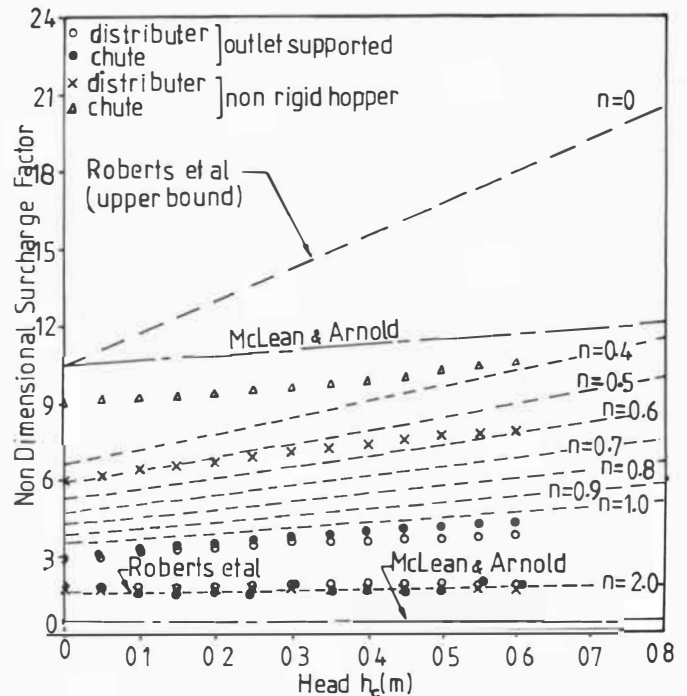


Fig. 10: Comparison of theoretical and experimental feeder loads in plane flow bin and belt feeder test rig — material: white sand

theory would indicate that feeder loads computed on the basis of Eqs. (24) or (25) with  $n = 0$  be regarded as a possible upper bound. A satisfactory prediction of initial loads can be made by using Eq. (24) with appropriate values of  $n$  from Table 1.

Table 1: Initial filling conditions

Clearance C mm	Method of Filling	Rate of Filling	Hopper Wall Type	n	K = K <sub>min</sub>
0	chute	fast	nonrigid	0.1—0.2	0.456—0.498
15	chute	fast	nonrigid	0.2—0.3	0.498—0.54
0	chute	slow	nonrigid	0.2—0.3	0.498—0.54
15	chute	slow	nonrigid	0.3—0.5	0.54 —0.623
15	chute + dist.	slow	nonrigid	0.7—0.9	0.69 —1.16
15	chute + dist.	fast	nonrigid	0.5—0.6	0.623—0.664

**7.2 Flow Conditions**

The theoretical predictions given by Eq. (27) underestimate the feeder loads. The comparison between the measured and predicted values based on the major consolidating pressure  $\sigma_1$  for which Eq. (29) applies is quite satisfactory (Figs. 9 and 10).

**8. Power to Shear Bulk Solid in Hopper**

The total load on the feeder is computed from Eq. (21) using the appropriate value of the surcharge factor  $q$  from Eq. (24).

For a belt or apron feeder, the force to shear the material is given by:

$$F = \mu_i Q \tag{30}$$

The value of  $\mu_i$  is given in Table 2.

Table 2: Values of  $\mu_i$

Researcher	$\mu_i$
Reisner [3], Bruff [4]	0.4
Johanson [5], McLean and Arnold [10]	$\sin\delta$
Rademacher [13]	$0.8 \sin\delta$

Following Rademacher [12] and considering the quasi-static equilibrium of the bulk solid at the interfacial zone, the following expression for  $\mu_i$  can be deduced:

$$\mu_i = \tan \left[ \xi + \tan^{-1} \left( \frac{T - F_s}{Q - w} \right) \right] \tag{31}$$

where:

- $\xi$  — release angle
- $T$  — tangential load
- $F_s$  — skirt friction
- $Q$  — initial load
- $w$  — weight of the interfacial material.

Table 3 presents experimental values of  $\mu_i$  obtained using Eq. (31).

Table 3: Experimental values of  $\mu_i$  obtained using Eq. (31)

Bulk Solid	Gate Height m	$\mu = \sin\delta$	$Q_i$ kN	$Q_{si}$ kN	$\mu_i$	$\mu_i/\mu$ %
Plastic pellets	0.02	0.6691	0.2524	0.1372	0.5433	81.15
	0.042	0.6691	0.2646	0.1176	0.461	69.02
	0.062	0.6691	0.2892	0.1367	0.514	76.8
	0.108	0.6691	0.2744	0.118	0.486	72.63

Current experimental investigations suggest that  $\mu = \sin\delta$  overestimates and  $\mu = 0.4$  underestimates the power requirements. Based on model analysis,  $\mu = \mu_i$  is calculated from Eq. (31). It is noticed from Table 3 that  $\mu_i = 0.7$  to  $0.8$  times  $\sin\delta$  is a reasonable prediction.

The power to shear bulk solid at the hopper outlet is given by:

$$P = Fv \tag{32}$$

In addition to this power, component resistances and corresponding powers due to such factors as belts, skirtplates and gates must also be taken into account; they are discussed in Section 12.

**9. Influence of Hopper Geometry on Feeder Loads — Effect of Varying  $\alpha$  and  $B$**

For reliable and uninterrupted flow, it is recommended that a mass flow hopper be employed. The flow rate from mass flow hoppers depends on the hopper geometry, the wall lining material and the flow properties of the bulk solid. As commonly occurs in practice, the wall friction angle  $\phi$  decreases with increase in the major consolidating pressure  $\sigma_1$ ; a decrease in  $\phi$  permits  $\alpha$  to increase. At the same time, an increase in  $\sigma_1$  in the flow stress field is accompanied by an increase in  $B$ . The net result is that the half-angle  $\alpha$  will normally increase with the opening dimension  $B$ , the rate of increase being more pronounced at low values of  $B$ , with  $\alpha$  approaching a constant value as  $B$  becomes larger, as shown in Fig. 11. For a plane flow hopper  $\alpha$  is about  $12^\circ$  larger than for a conical hopper for the same value of  $B$ . The potential flow rate is quite significant, and while in some operations there is a need for high discharge rates, for the majority of cases the potential flow rate may be excessive, rendering the need to employ feeders as flow controlling devices.

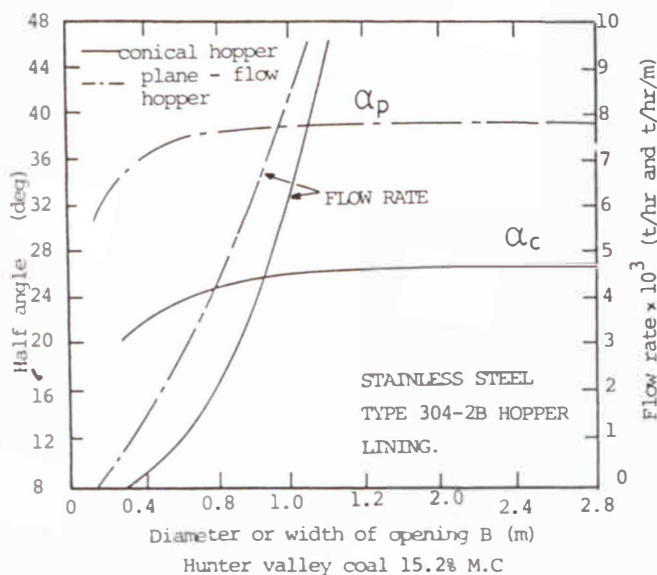


Fig. 11: Mass flow hopper geometries and flow rates for typical coal

By way of example, consider the wedge-shaped plane flow bin and belt feeder of Fig. 12. The bin, which is to handle

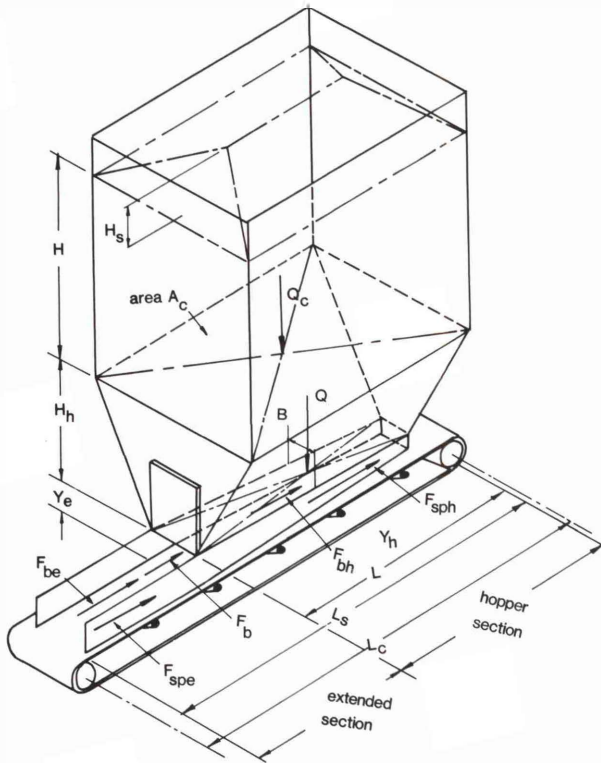


Fig. 12: Schematic arrangement of wedge-shaped bin and belt feeder

coal, is of mild steel, with the hopper being lined with stainless steel type 304 with 2B finish. The relevant details are:

1. Bin

Height $H$	8.0 m
Width $D$	5.0 m
Length $L$	5.0 m
Surcharge $H_s$	1.5 m

The hopper height  $H_h$ , half-angle  $\alpha$  and opening dimension  $B$  are to be varied in accordance with the flow properties of the coal.

2. Coal

Effective angle of internal friction $\delta$	50°
Angle of friction between coal and mild steel $\phi$	30°
Angle of friction between coal and stainless steel $\phi$	18°
Bulk density $\rho$	0.95 t/m <sup>3</sup>

The coal flow properties permit  $\alpha$  and  $B$  to be varied in accordance with Fig. 13. The changes in surcharge factors  $q_i$  and  $q_{f\sigma_1}$  are also shown in Fig. 13;  $q_i$  has been determined using Eq. (25). The feeder loads  $Q_i$  and  $Q_{f\sigma_1}$  determined in accordance with the methods outlined are shown plotted in Fig. 13. The decrease in  $Q_i$  and  $Q_{f\sigma_1}$  with increase in  $\alpha$  and  $B$  to maintain mass flow is clearly evident. However, the ratio  $Q_i/Q_{f\sigma_1}$  increases with decrease in  $B$ .

10. Controlling the Feeder Loads

Once the flow has been initiated and the feeder stopped, the load on the feeder does not revert to the original initial load, but remains almost equal to the flow load during which an arched stress field exists. This concept leads to the genera-

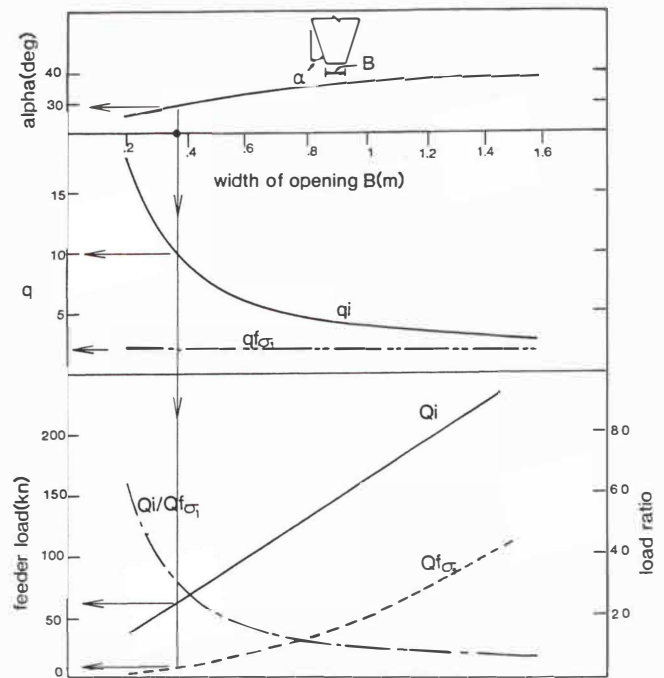


Fig. 13: Feeder load variations with hopper geometry for plane flow bin example

tion and maintenance of an arched stress field in the hopper during filling. The methods proposed to control the feeder loads, with each method having been thoroughly investigated, are:

1. Slow feeder motion during filling
2. Feeder flexibility
3. Retaining a cushion of material.

10.1 Slow Feeder Motion during Filling

Slow motion of the feeder is possible in all the feeders with stepped speed control, and it is a simple means of controlling the feeder loads. Fig. 14 shows that the loads generated during filling are almost equivalent to the loads during flow. Even a slight motion of the material is enough to create an arched stress field in the hopper section.

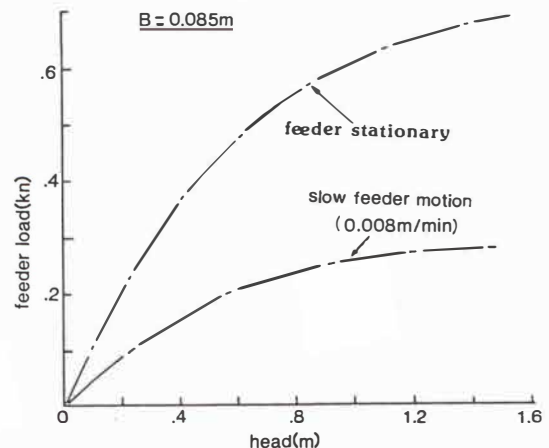


Fig. 14: Reduction of initial feeder load due to very slow running of the feeder during filling for the model test rig

**10.2 Feeder Flexibility**

The loads which act on the feeders are very much dependent on the clearance between the hopper outlet and the feeder and the flexibility of the feeder supports. If the feeder is firmly attached to the hopper and the bulk solid within the feeder is contained by closely fitted skirts, the load is close to the hydrostatic value. If the feeder supports are flexible and deflect more than the hopper as the bin is filled, the loading on the feeder is significantly reduced, as shown in Fig. 15. The slight movement of the material when the feeder is displaced is equivalent to some of the material being withdrawn from the hopper, and the loading shifts partly towards dynamic values.

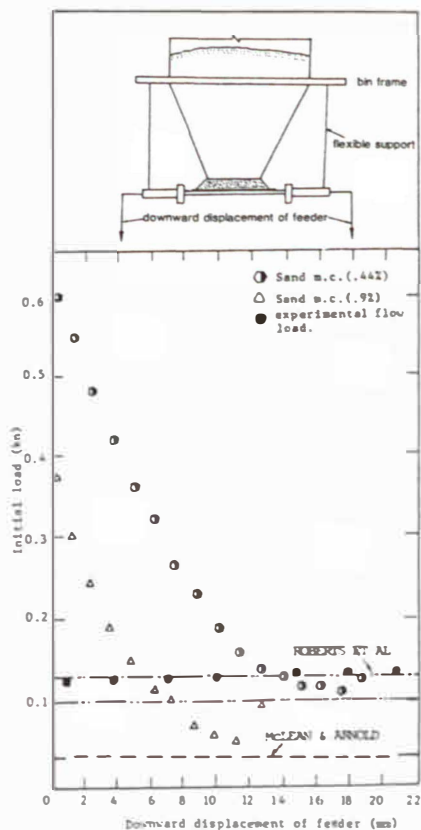


Fig. 15: Reduction of initial feeder load due to downward displacement of the feeder

**10.3 Effects of Cushioning**

The high initial loads which act on feeders are a matter of some concern, and possible steps should be taken to reduce the magnitude of these loads, which has been demonstrated by Roberts et al. [26]. Fig. 16 presents experimental results for the model plane flow bin and belt feeder using sand. Computed nondimensional surcharge factors are compared with the theoretical results. The reduction of the initial loads due to cushioning is quite significant. This is because the material left in the hopper, having previously been in motion, will preserve an arched stress field. The new material being deposited will have a peaked stress field. This will provide a surcharge load on the arched stress field, but the magnitude of the load at the outlet will be of a lower order than if the bin is totally filled from empty condition. It is noticed that the experimental values are higher than the theoretical curve as

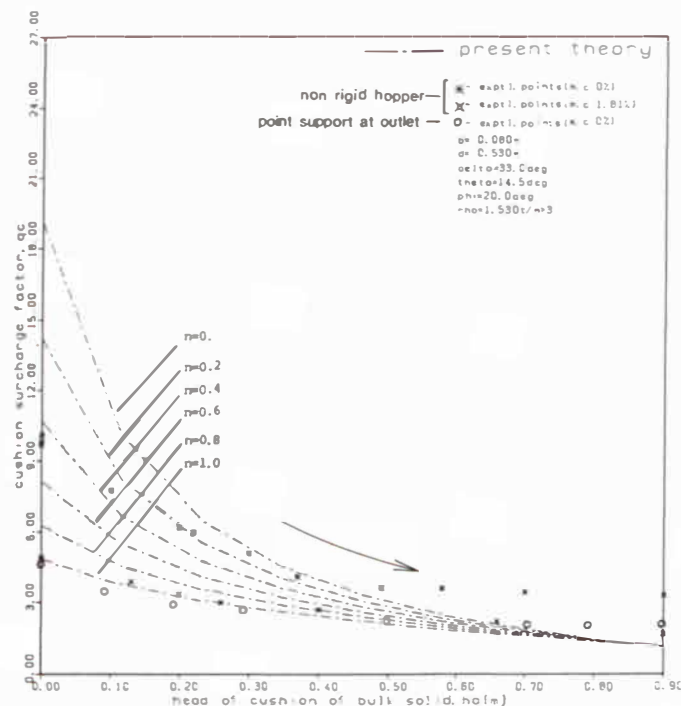


Fig. 16: Influence of "cushioning" on initial feeder loads

the head  $h_a$  of the cushion of bulk solid is increased. This is certainly due to the redistribution of the stress field at the interfacial zone of the hopper and feeder. Further, the theoretical analysis does not take into account the acceleration of the layer [15]; the increase in the bulk density of the flowing bed due to sudden stoppage of the feeder results in higher loads than the fully developed dynamic values. In the theoretical analysis, the material is assumed to be fully plastic, which gives rise to lower bound values. The other reason being the clearance between the feeder and the hopper outlet, the material weight in this interfacial zone and on the feeder has to be considered. Hence a correction factor is introduced which takes account of the weight of the material in the interfacial zone and on the feeder and the rate of change of the momentum during filling the bin.

The condition for the minimum height of cushion is given by:

$$\frac{dp_v}{dz} = 0 \tag{33}$$

Based on this, it is possible to derive an expression for the minimum height of the cushion to achieve almost flow loading conditions:

$$z \leq h_0 - n q_{t0_1} (4/\pi)^m B \tag{34}$$

where the value of  $n$  is to be computed from  $K = K_{max}$  and  $q_{t0_1}$  is given by Eq. (24).

**11. Effect of Hopper Wall Rigidity on Feeder Design**

The hopper wall deflection is proportional to the head of the bulk solid contained within. Accordingly, the hopper walls are classified into rigid and nonrigid types, based on the magnitude of the normal wall stress  $p_n$  exerted on them

being hydrostatic or less. Static stresses more than hydrostatic are physically not possible. Based on the experimental investigations, it is found that the feeder load and power requirements reduce significantly as the hopper wall becomes nonrigid, forcing the channel boundary to be flexible. This results in economical and less troublesome feeder design and performance requirements. Further, any deflection of the hopper wall before start-up to relieve the arches at the outlet has a detrimental effect on the operation and maintenance of the feeder, and the initial load and power requirement to shear the bulk solid at least doubles. This is due to sudden slippage of bulk solids at the walls, which acts as shock loading on the feeder. Fig. 17 shows the effects of rigidity on wall pressures and feeder loads.

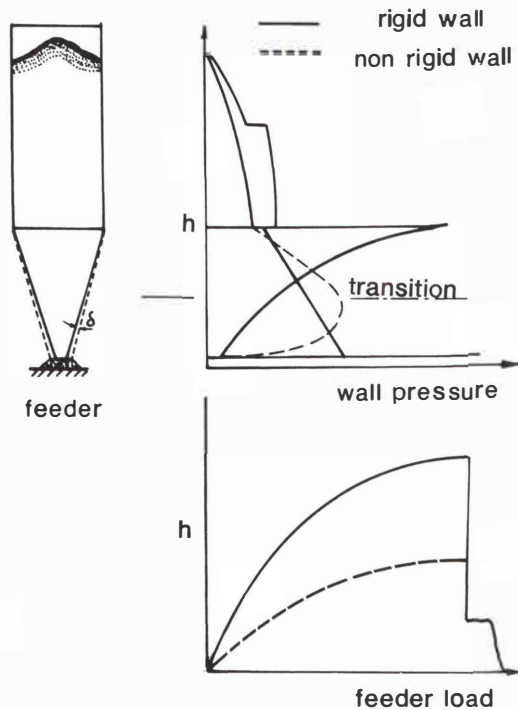


Fig. 17: Effect of rigidity of the hopper wall on wall pressures and feeder loads

By way of illustration, Fig. 18 shows the predicted wall pressures, based on a rigid hopper, and the corresponding measured values for the model plane flow bin and feeder of Fig. 3. Despite the fact that the hopper walls of the model were well supported, a small amount of movement did occur. This explains why the initial pressures in the hopper vary from the hydrostatic based values, particularly towards the hopper outlet where the measured values are significantly lower. The measured flow pressures also show a departure from the predicted values, being lower towards the transition and higher towards the outlet. Other tests using the model bin in which the walls had greater flexibility have indicated a more pronounced "bulge" in the initial pressure curve of the type illustrated in Fig. 17.

## 12. Total Power Requirements for Belt Feeders

For a complete feeder design, the total power for the initial and flow cases needs to be determined. In addition to the

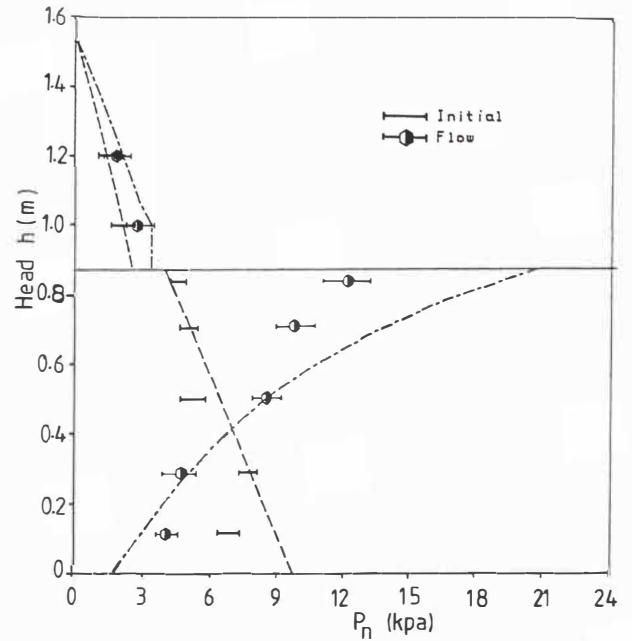


Fig. 18: Normal wall pressure measurement, initially and during flow — bin:  $D = 0.53$  m,  $B = 0.08$  m,  $H = 0.63$  m; material:  $\delta = 33^\circ$ ,  $\phi = 20^\circ$ ,  $\rho = 1.52$  t/m<sup>3</sup>

feeder loads and the corresponding power to "shear" the bulk solid, consideration will need to be given to the other resistances to be overcome in order to operate the feeder. In the case of belt feeders, for example, the influence of skirt-plates and belt resistances must be taken into account, and this is illustrated by a design example in Section 12.2.

### 12.1 Design Equations for Belt Feeders

By way of illustration, the power requirements for a dump hopper and belt feeder of the type illustrated in Fig. 12 are now considered. The design equations are summarised in the following [26].

#### 12.1.1 Bin and Hopper Surge and Corresponding Power

These are determined in accordance with the methods described in Section 6.

#### 12.1.2 Skirtplate Resistance

Assuming steady flow, the skirtplate resistance is determined for the hopper section and for the extended section (see Fig. 12). The pressure distributions for the skirtplate sections are illustrated in Fig. 19.

Neglecting the vertical supports  $y_h$  and  $y_e$  due to the skirt-plates, the skirtplate resistance is given by:

— for the hopper section:

$$F_{sph} = \mu_2 K_v (2Q + \rho g B L y_h) y/B \quad (35)$$

— for the extended section (section beyond hopper):

$$F_{spe} = \mu_2 K_v \rho g (L_s - L) y_e^2 \quad (36)$$

where:

- $Q$  — feeder loads as determined by Eq. (21)
- $\rho$  — bulk density

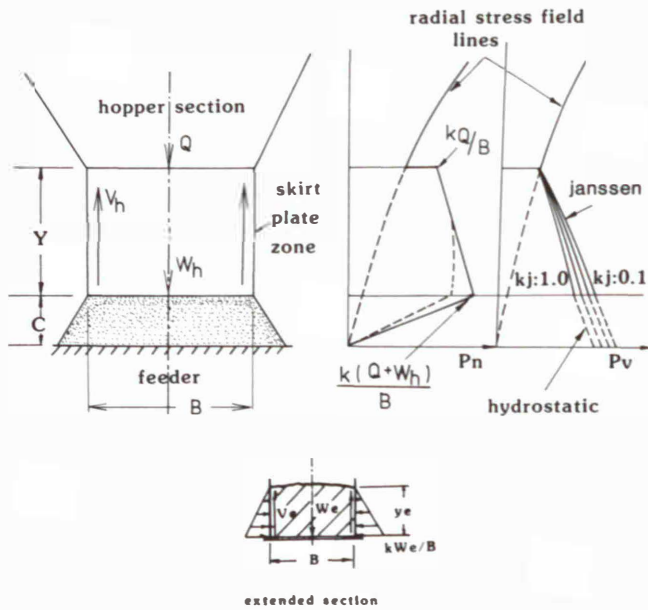


Fig. 19: Skirt zone pressure distributions

- $y_h$  — average height of material against skirtplates for hopper section
- $y_e$  — average height of material against skirtplates for extended section
- $K_v$  — ratio of lateral to vertical pressure at skirtplates
- $g$  — acceleration due to gravity;  $g = 9.81 \text{ m/s}^2$
- $B$  — width between skirtplates
- $\mu_2$  — skirtplate friction coefficient
- $L_s$  — total length of skirtplates.

The pressure ratio  $K_v$  is such that  $0.4 \leq K_v \leq 1.0$ . The lower limit may be approached for the static case and the upper limit for steady flow.

**12.1.3 Belt Load Resistance**

The belt load resistance is given by:

— for the hopper section:

$$F_{bh} = (Q + \rho g B L y) \mu_b \tag{37}$$

— for the extended section:

$$F_{be} = \rho g B (L_s - L) y \mu_b \tag{38}$$

where:

$\mu_b$  — idler friction;  $\mu_b \approx 0.02$ .

**12.1.4 Empty Belt Resistance**

$$F_b = w_b L_b \mu_b \tag{39}$$

where:

$w_b$  — belt weight per unit length  
 $L_b$  — total length of belt.

**12.1.5 Force to Accelerate Material onto Belt**

$$F_A = Q_m v \tag{40}$$

where:

$Q_m$  — mass flow rate  
 $v$  — belt speed.

It is assumed that:

$$Q_m = \rho B y v \tag{41}$$

Usually, the force  $F_A$  is negligible.

**12.1.6 Initial and Flow Loads and Powers**

The foregoing loads and resistances are determined for the initial and flow conditions using the appropriate values of the variables involved.

The power is computed from:

$$P = (\sum \text{Resistances}) \frac{v}{\eta} \tag{42}$$

where:

$\eta$  — efficiency  
 $v$  — belt speed.

The condition for non-slip between the belt and the bulk solid under steady motion can be determined as follows:

$$\mu_3 (Q_f + W) \geq F_f + F_{sp} \tag{43}$$

where:

$\mu_3$  — coefficient of friction between belt and bulk solid  
 $Q_f$  — flow surcharge at hopper outlet  
 $W$  — weight of bulk material between skirtplates in hopper section of conveyor  
 $F_f$  — force to shear material at hopper outlet  
 $F_{sp}$  — skirtplate resistance.

A design example is presented in the next section, taking into account the above design equations.

**12.2 Design Example — Feeder Loads and Power Determination [26]**

**12.2.1 Design Data**

*Bin Details:*

Type of hopper	plane flow
Hopper opening dimension $B$	1.50 m
Bin diameter or width $D$	5.00 m
Height of cylinder $H$	8.00 m
Cylinder surcharge $H_s$	1.50 m
Height of hopper $H_h$	2.50 m
Hopper half-angle $\alpha$	35°
Length of outlet slot $L$	5.00 m

*Belt Feeder Details:*

Feeder speed $v$	0.50 m/s
Length of skirtplate $L_s$	20.00 m
Average height of skirtplate $z$	0.50 m
Pressure ratio $K$ for initial case	0.40
Pressure ratio $K$ for flow, hopper section	1.00
Pressure ratio $K$ for flow, belt section	1.00
Length of feeder $L_b$	20.00 m
Belt width $B_b$	2.00 m
Drive efficiency $E_{ta}$	90 %
Skirtplate friction angle $\phi_s$	30°
Belt idler friction coefficient $U_b$	0.03

*Bulk Solid Flow Properties:*

Effective angle of internal friction $\delta$	50°
Wall friction angle for cylinder $\phi_c$	30°
Wall friction angle for hopper $\phi_h$	18°
Bulk density $\rho$	0.95 t/m <sup>3</sup>

12.2.2 Feeder Loads and Power Requirements

*Hopper Surcharge, Loads and Power:*

Bin surcharge $Q_c/A_c$	40.53 kPa
Initial surcharge factor $q_i$	2.54
Flow surcharge factor $q_f$	1.05
Feeder load, initial condition, $Q_i$	265.89 kN
Tangential load, initial condition, $F_i$	162.94 kN
Feeder load, flow condition, $Q_f$	109.84 kN
Tangential load, flow condition, $F_f$	67.31 kN
Feeder power, initial condition, $P_i$	81.47 kW
Feeder power, flow condition, $P_f$	33.66 kW

*Skirtplate and Belt Resistances:*

Skirtplate resistance, initial condition:	
— hopper section, $F_{sph,i}$	43.63 kN
— extended section, $F_{spe,i}$	8.07 kN
Belt load resistance, initial condition:	
— hopper section, $F_{bh,i}$	9.03 kN
— extended section, $F_{be,i}$	3.15 kN
Skirtplate resistance, flow condition:	
— hopper section, $F_{sph,f}$	49.00 kN
— extended section, $F_{spe,f}$	20.18 kN
Belt load resistance, flow condition:	
— hopper section, $F_{bh,f}$	4.34 kN
— extended section, $F_{be,f}$	3.15 kN
Empty belt resistance $F_b$	1.41 kN
Force to accelerate material $F_a$	0.09 kN

*Total Resistance and Power for Belt Feeder:*

Total resistance, initial, $F_{tot,i}$	229.73 kN
Total resistance, flow, $F_{tot,f}$	146.90 kN
Total power, initial, $P_{tot,i}$	127.63 kW
Total power, flow, $P_{tot,f}$	81.61 kW

**13. Summary of Conclusions**

Based on the work reported in this paper, the following conclusions may be stated:

1. To achieve the most reliable feeding of bulk solids, mass flow hoppers should be used in conjunction with feeders. This will ensure reliable flow, provided the feeder geometry is such that uniform draw of material is achieved with a fully active hopper outlet.
2. Eq. (24) is recommended for determining the initial loads on feeders, provided an appropriate value of  $n$  is used. However, for simplicity, Eq. (26) may also be used.
3. Eq. (29) is recommended to compute the loads on feeders under flow conditions.
4. In order to reduce feeder loads and the corresponding power requirements during start-up, some form of cushioning in the hopper is recommended. Also, nonrigid skirt zones may be employed in order to reduce feeder loads. Methods of controlling feeder loads are discussed in Section 10.

5. The value of  $\mu_i = 0.8 \sin \delta$  is recommended to calculate the force to shear the bulk solid in the hopper.

**Acknowledgements**

The advice and assistance rendered by Mr. Ooms of the University of Newcastle in the experimental work throughout the investigation is gratefully acknowledged. Finalisation of the writing of this paper was undertaken at the University of Twente in The Netherlands during a period of Research Fellowship of the second named author. Appreciation is expressed to the University of Twente for the opportunity provided.

**References**

- [1] Jenike, A.W.: Storage and Flow of Solids. Bull. 123, Utah Eng. Exp. Station, University of Utah, 1964.
- [2] Hager, M.: Untersuchungen zur Befüllung und zum Gutaustag von Bunkern mit Abzugsbändern (Investigations on the Feeding and Recovery of Bulk Materials from Bunkers with Belt Conveyors). Dr. Thesis, Technical University Hannover, 1965 (in German).
- [3] Reisner, A., and M. von Eisenhart Rothe: Bins and Bunkers for Handling Bulk Materials. Trans Tech Publications, Clausthal-Zellerfeld, Federal Republic of Germany, 1971.
- [4] Bruff, W.: Industrisiloer. Ingeniorforlaget A/S, 1974 (in Norwegian).
- [5] Johanson, J.R.: Storage and Flow of Solids. Three-Day Working Seminar Notes, Australian Mineral Foundation, Adelaide, July 1976.
- [6] Rawlings, R.A.: The Importance of Efficient Feeder Design; Bulk (1977) July/Aug.
- [7] Wright, H.: BSC's Contribution to the Design and Operation of Mass Flow Bunkers; Iron and Steel Int. (1978) Aug., pp. 233—238.
- [8] Colijn, H., and P.J. Carroll: Design Criteria for Bin Feeders; Trans. SME-AIME Vol. 241 (1968) Dec., pp. 389—404.
- [9] Colijn, H., and E.A. Vitunac: Application of Plow Feeders. Annual Winter Meeting, ASME, New York, Dec. 2—7, 1979, Paper 79-WA/MH-1.
- [10] McLean, A.G., and P.C. Arnold: A Simplified Approach for the Evaluation of Feeder Loads for Mass Flow Bins; J. Powder and Bulk Solids Technology Vol. 3 (1979) No. 3, p. 25—28.
- [11] Arnold, P.C., A.G. McLean and A.W. Roberts: Bulk Solids: Storage, Flow and Handling. The University of Newcastle Research Associates (TUNRA) Ltd., 2nd Ed., 1982.
- [12] Rademacher, F.J.C.: Feeders and Vibratory Conveyors. TUNRA Bulk Solids Handling Research Associates.
- [13] Rademacher, F.J.C.: Reclaim Power and Geometry of Bin Interfaces in Belt and Apron Feeders; bulk solids handling Vol. 2 (1982) No. 2, pp. 281—294.



- [14] Johanson, J.R.: Stress and Velocity Fields in the Gravity Flow of Bulk Solids; *J. Appl. Mech.* (1964).
- [15] Enstad, G.G.: A Novel Theory of Arching and Doming in Mass Flow Hoppers. The Chr. Michelsen Inst., Dept. of Science and Technology, Bergen 1981.
- [16] Walters, J.K.: A Theoretical Analysis of Stresses in Axially-Symmetric Hoppers and Bunkers; *Chem. Eng. Science* Vol. 28 (1973).
- [17] Floating Pressure Cells with Keller Transducers. Series S, No. 8440, Dept. of Struct. Eng., Technical University of Denmark.
- [18] Arnold, P.C.: Feeding of Bulk Solids onto Conveyor Belts — Feeders and Feeder Loads. Symp. on Belt Conveying of Bulk Solids, TUNRA Bulk Solids Handling Research Associates, The University of Newcastle, Nov. 1982.
- [19] Roberts, A.W.: Feeding of Bulk Solids onto Conveyor Belts — Transfer Chute Performance and Design. Symp. on Belt Conveying of Bulk Solids. TUNRA Bulk Solids Handling Research Associates, The University of Newcastle, Nov. 1982.
- [20] Roberts, A.W., P.C. Arnold, A.G. McLean and O.J. Scott: The Design of Gravity Storage Systems for Bulk Solids; *Trans. Inst. of Eng. Australia, Mechanical Engineering*, Vol. ME7 (1982) Nr. 3.
- [21] Wilms, H., and J. Schwedes: Reclaim Power for Coal Bunkers. I. *Chem. E. Symp.*, Series No. 69.
- [22] Roberts, A.W.: Design and Application of Feeders for the Controlled Loading of Bulk Solids onto Conveyor Belts. *Proc. Beltcon 2, Int. Conf. on Materials Handling*, Johannesburg, May 1983.
- [23] Jenike, A.W.: Load Assumptions and Distributions in Silo Design. *Conf. on Construction of Concrete Silos*, Oslo, Jan. 1977.
- [24] McLean, A.G.: Content Generated Loads on Bins and Silos. Post-graduate Workshop on Design of Steel Bins for the Storage of Bulk Solids, University of Sydney, March 1985.
- [25] Jenike, A.W., J.R. Johanson and J.W. Carson: Bin Loads — Part 3: Mass Flow Bins; *Trans. ASME., J. Eng. for Industry*, Series B, Vol. 95 (1973) No. 1.
- [26] Roberts, A.W., M. Ooms and K.S. Manjunath: Feeder Load and Power Requirements in the Controlled Gravity Flow of Bulk Solids from Mass Flow Bins; *Trans. Inst. of Eng. Australia*, Vol. ME9 (1984), pp. 49—61.